Effect of Prior Ratcheting Deformation on Low Cycle Fatigue Behaviour of AISI 4340 Steel

Krishna Dutta[(⊠)] and K. Divya Bharathi

Department of Metallurgical and Materials Engineering,
National Institute of Technology Rourkela, Rourkela 769008, India
duttak@nitrkl.ac.in

Abstract. Fatigue damage of a material is particularly deleterious when it occurs under asymmetric cyclic loading conditions. Ratcheting is the process of fatigue damage in which plastic strain accumulates during asymmetric cyclic loading (with non-zero mean stress) of structural parts. The aim of this investigation was to study the ratcheting behaviour and its effect on strain-controlled low cycle fatigue (LCF) behaviour of AISI 4340 steel in differently heat treated conditions. For this purpose, AISI 4340 steel was first given different heat treatments viz. annealing and normalizing and studied for basic microstructural characterizations and hardness. The heat treated steel rods were used to fabricate tensile and fatigue specimens according to ASTM standards. A series of stress controlled ratcheting tests were carried out on the heat treated specimens at room temperature with different stress ratios (R) of −0.4, −0.6 and −0.8. In order to assess imposed fatigue damage, post-ratcheting LCF studies were done on the annealed specimens. The results showed that accumulation of ratcheting strain increased with increasing stress ratios in both annealed and normalised conditions. Maximum accumulation of ratcheting strain (1.16% for annealed and 1.02% for normalised specimens) was observed at R = −0.4. The increase in strain accumulation with increasing stress ratio can be attributed to the increased dislocation generation and their multiplication, at higher levels of stress ratios. Post-ratcheting LCF studies indicated increased stress amplitudes of the ratcheted specimens as those compared to only LCF specimens; this can be attributed to the previous cyclic hardening during ratcheting tests.

Keywords: AISI 4340 steel · Ratcheting · Post-ratcheting LCF

1 Introduction

The ratcheting phenomenon is considered as the cyclic plastic deformation of materials, [1]. It occurs under the influence of positive or negative mean stress i.e. when components are subjected to asymmetric cyclic loading. Accumulation of ratcheting strain can significantly reduce the fatigue life of a component [2]. In practice, both ratcheting and fatigue can simultaneously be imposed on engineering components and thus failure may occur due to both of these. Therefore, it is of significant importance to understand effect of ratcheting deformation on final properties of a material before the designing in order to assess its proper fatigue life and more importantly, to avoid catastrophic failure.

AISI 4340 steel is traditionally used in aerospace, automotive industries; the steel is known to be provided with normalising heat treatment before being designed to any component [3]. In the above-mentioned sectors, the occurrences of ratcheting deformation cannot be ruled out. Further, both ratcheting and conventional low cycle fatigue damage may still deteriorate the situation. A few recent reports examined the ratcheting and ratcheting induced tensile damage in structural materials [4–8]. However, ratcheting behaviour of AISI 4340 steel in different heat treatment conditions were not reported. Further, effect of previous ratcheting on conventional low cycle fatigue behaviour of the steel was also not reported. Therefore, in the present work, effect of stress ratio on ratcheting behavior of AISI 4340 steel was studied in annealed and normalised conditions. Post ratcheting low cycle fatigue (LCF) behaviour was investigated in order to substantiate effect of previous ratcheting deformation on it.

2   Experimental Details

2.1   Material Selection, Heat Treatment, Basic Metallography and Specimen Design

The selected steel for this investigation was available in the form of extruded rods of 18 mm diameter. The chemical composition of the steel is (in wt%): C – 0.35, Ni – 1.52, Cr – 1.44, Mo – 0.18, Mn – 0.69, Si – 0.31, S – 0.02, P – 0.03 and balance Fe. The as-received rods were subjected to annealing and normalising heat treatments by soaking at 750 °C and 870 °C respectively followed by furnace cooling and air cooling. The soaking time was 2 h. Specimens with approximate height of 10–12 mm were cut from the heat treated rods for microstructural characterizations and determination of hardness. The microstructural studies of the steel were carried out using an optical microscope (Carl Zeiss, Germany) connected to an image analyzer (Software: Axiovision). The hardness values of the differently heat treated specimens were measured using Vickers hardness tester (LECO LV400, US) at an indentation load of 20 kgf with dwelling time of 15 s. Tensile and fatigue test specimens were fabricated following ASTM standards E8M [9] and E-606 [10] respectively from heat treated rods. Schematic diagrams of the tensile and fatigue specimens are illustrated in Fig. 1. The tensile tests were done using a servo hydraulic universal testing machine (BISS, India) of capacity ±100 kN, at a cross head velocity of 1 mm/min.

2.2   Ratcheting and Post-ratcheting Low Cycle Fatigue Tests

All the stress-controlled low cycle fatigue i.e. ratcheting tests were carried out using the universal testing machine mentioned above at different stress ratios and at room temperature. The stress rate was maintained as 50 MPa/s. The various stress ratios and their corresponding stress amplitude (σ_a) and mean stress (σ_m) values are summarized in Table 1.

During the tests, the load and extension data were recorded continuously by using the attached software to a computerized console. Further, the strain data were recorded using a 12.5 mm dynamic extensometer. It was aimed to acquire at least 250 data
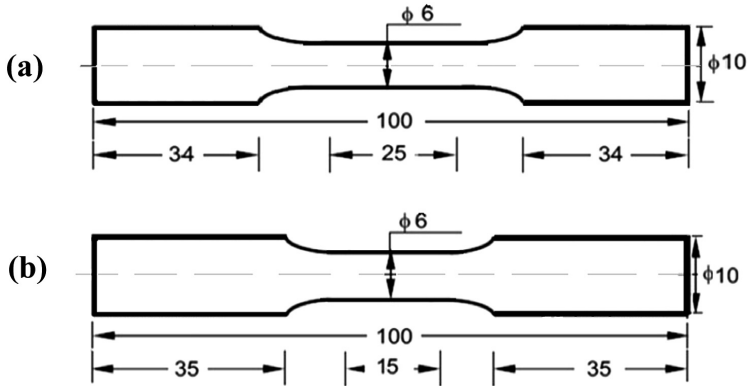
Fig. 1. Typical configuration of the specimens used for (a) tensile and (b) fatigue tests. Here, all dimensions in the figures are in mm.

Table 1. The stress parameters for ratcheting tests.

Stress ratio (R)	Annealed		Normalised	
	σ_m (MPa)	σ_a (MPa)	σ_m (MPa)	σ_a (MPa)
−0.4	240	560	390	910
−0.6	160	640	260	1040
−0.8	80	720	130	1170

points per cycle during the tests. All the ratcheting tests were done up to 100 cycles. Post-ratcheting strain-controlled low cycle fatigue tests were done on the ratcheted specimens after completion of these tests.

One set of annealed specimens were studied for only strain-controlled low cycle fatigue tests (for strain amplitudes of ±0.50 and ±0.75) up to 100 cycles and another set of specimens were subjected to strain-controlled tests after previous ratcheting (stress-controlled, at $R = −0.4$). The strain-controlled tests were done at strain rate of $0.08\ \text{s}^{-1}$.

3   Results and Discussion

3.1   Microstructural Analysis

The optical microstructures of the investigated material in annealed and normalised conditions are shown in Fig. 2(a) and (b) respectively. The annealed microstructure as in Fig. 2(a) is composed of ferrite (light) and pearlite (dark). Figure 2(b) shows the optical microstructure of normalised AISI 4340 steel. It consists of finer grains compared to the annealed one, as expected. The faster rate of cooling during normalising led to the formation of fine-grained microstructure. The grain sizes were estimated using linear intercept method following ASTM E112 [11]. Average grain size of the

steel was found to be 16.55 ± 2.07 μm and 7.20 ± 1.14 μm for annealed and normalised specimens respectively.
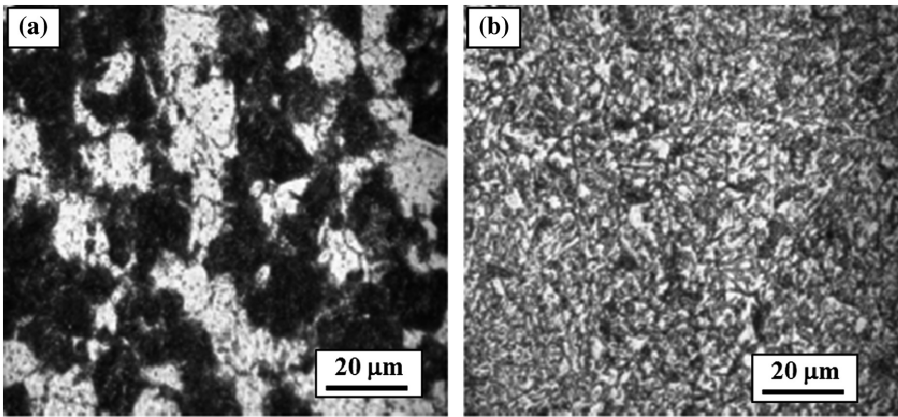

Fig. 2. Optical microstructures of the investigated AISI 4340 steel at (a) annealed and (b) normalised heat treatment condition

3.2   Hardness and Tensile Properties

The average Vickers hardness of the steel was 228 ± 1.13 and 321 ± 1.17 in annealed and normalised conditions respectively. These results are in accordance with that provided in ASM Handbook [3]. Typical engineering stress-engineering strain diagrams for the investigated steel for annealed and normalised specimens are illustrated in Fig. 3. In both the cases, a continuous transition from elastic to plastic region were noticed and therefore the yield strength was estimated by 0.2% strain off-set method, following ASTM E8M [9]. The tensile properties of the steel are provided in Table 2. The strain hardening exponent (n) of the steel was estimated by calculating the true stress (σ) and true strain (ε) values from the engineering stress and engineering strain respectively. The strain hardening exponent values were calculated (in the strain range of 1.68 to 4.13 for annealed, 1.11 to 2.88 for normalised samples) by using Hollomon equation $\sigma = K\varepsilon^{n}$, where K is strength coefficient.

3.3   Ratcheting Behavior Under Varying Stress Ratios

The detailed results of all the ratcheting tests conducted up to 100 cycles were reported elsewhere [8]. It was evident that the stress – strain hysteresis loops shifted towards positive strain direction upon successive cycling of ratcheting. It is the indicative for accumulation of plastic strain to the material. In this investigation, the extent of accumulation of ratcheting strain was calculated by taking the average of minimum and maximum strain in particular cycle.

During the ratcheting deformation it is usually noticed that the strain range changes with progression of cycles; it is considered to happen due to the change in hardening or
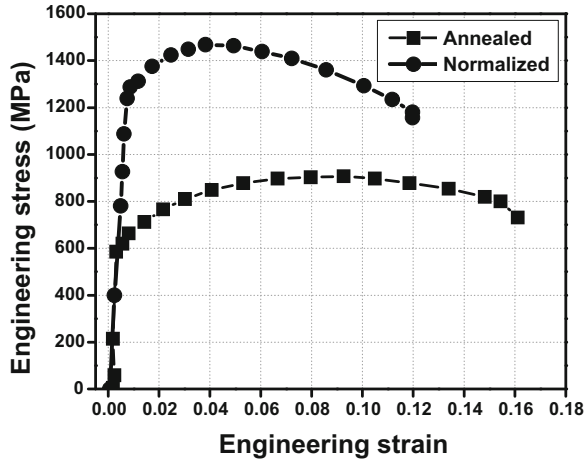
Fig. 3. Engineering stress strain curve for annealed and normalised samples of AISI 4340 steel.

Table 2. Tensile properties of annealed and normalised samples of AISI 4340 steel.

Tensile parameter	Annealed	Normalised
Yield strength (MPa)	616	1300
Ultimate tensile strength (MPa)	906	1467
Strain hardening exponent (n)	0.18	0.10
Uniform elongation (ε_u) %	8.86	4.62
Total elongation (ε_t) %	16.11	11.94

softening response of the material. Kang et al. [12] reported that with the increase in ratcheting strain the stress–strain hysteresis loops become wider, if the material is cyclically softenable. As one can visualize, at constant stress range if higher amount of strain is produced in each successive cycle, cyclic softening takes place while the opposite is true for cyclic hardening [12, 13]. In the current investigation, the loop area decreased from first cycle to last cycle i.e., the strain accumulation is decreased from first to last cycle [8]. This fact indicates that the selected material is cyclically hardenable in nature.

Yoshida [14] studied the effect of stress ratio on ratcheting behaviour of SUS304 stainless steel. They reported that the strain accumulation increases with increasing stress ratio, but becomes negligible at R = −1. The variations of total accumulated ratcheting strain with stress ratio in AISI 4340 steel for the current investigation are illustrated in Fig. 4. As the stress ratio increases, ratcheting strain increase in both annealed and normalised samples, similar to the report published by Yoshida [14]. At a particular maximum stress, if the stress ratio (−ve) increases (e.g. here from −0.8 to −0.4), the minimum stress also increases (i.e., it becomes less negative). During loading in ratcheting experiments, dislocations generate in the substructure of the specimen in tensile loading direction. A part of this generated dislocations annihilate in

the reverse loading. If now the extent of reverse loading becomes large, significant amount of dislocations could be annihilated. Thus, the extent of residual dislocations is more while the minimum stress is more negative and that in turn for high stress ratio. The increase in strain accumulation with increasing stress ratio hence can be considered to happen because of increasing dislocation density, at higher stress ratio levels.
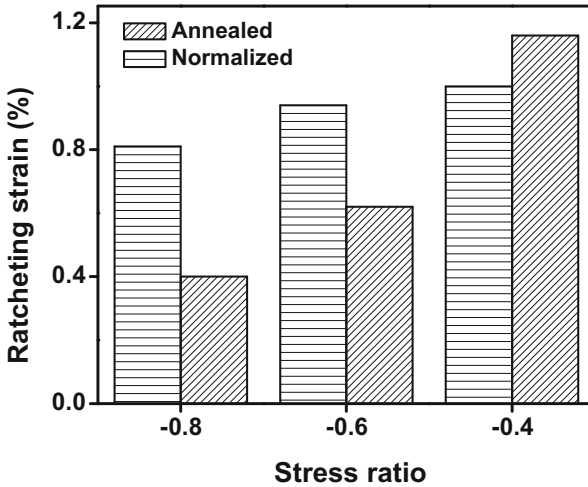

Fig. 4. Effect of stress ratio on accumulation of ratcheting strain.

3.4 Effect of Previous Ratcheting Deformation on Low Cycle Fatigue Behaviour of the Steel

It is known that ratcheting deformation causes plastic damage to a material and thus, it affects the properties of the material. To see the effect of previous ratcheting on the low cycle fatigue behaviour of the investigated material, one set of samples were tested for strain-controlled low cycle fatigue tests and another set of samples were first ratcheted up to 100 cycles followed by strain-controlled low cycle fatigue tests; both types of results are compared in terms of obtained stress amplitudes. The LCF tests were carried out at strain amplitudes of ± 0.50 and ± 0.75 whereas the ratcheting tests done at stress ratio of -0.4. In case of strain-controlled low cycle fatigue, cyclic hardening/softening would lead to increased/decreased peak stress with increasing cycles, respectively [1]. Figure 5(a) and (b) represent the hysteresis loops of 1st, 50th and 100th cycles, which were produced during strain-controlled tests for the annealed AISI 4340 steel at strain amplitudes of ± 0.50 and ± 0.75 respectively. The loop heights increased from 1st cycle to the last cycle indicating cyclic hardening.

Paul et al. [15] reported that with increasing applied strain amplitude, the degree of cyclic hardening initially increases and saturates at higher strain amplitude. Figure 6(a) and (b) display the variations of obtained stress amplitude with number of cycles for only strain-controlled LCF and post ratcheting LCF specimens, respectively. It was noted that for annealed AISI 4340 steel, the stress amplitudes in the cyclic straining
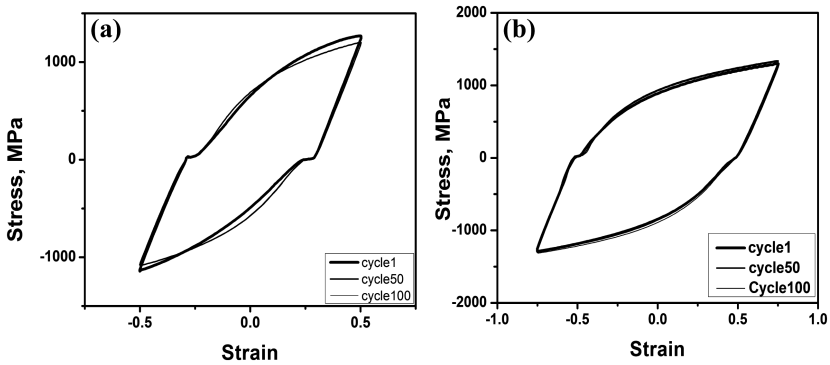
Fig. 5. Hysteresis loops produced during strain-controlled low cycle fatigue tests at strain amplitudes of (a) ±0.50 (b) ±0.75 for the annealed AISI 4340 steel.

with different applied strain amplitudes are different. The stress amplitude obtained as 1217 MPa and 1323 MPa at strain amplitudes of ±0.50 and ±0.75 respectively. At higher levels of cyclic straining (i.e., at ±0.75), hardening is rapid in the first few cycles, followed by an almost steady but low rate of hardening. It may be noted that complete saturated state of hardening was not exhibited. Similar dependency of cyclic hardening on imposed strain amplitude was also reported for different materials [15–17]. Overall, it was noticed that the required stress amplitudes were more for the ratcheted specimens as those compared with the only LCF specimens. The results indicated that almost 10% increment in peak stress took place for the lower strain amplitude test while the increment in peak stress was 7% for higher strain amplitude specimen. Thus it may be inferred that previous ratcheting deformation caused plastic damage to the specimens due to cyclic hardening.
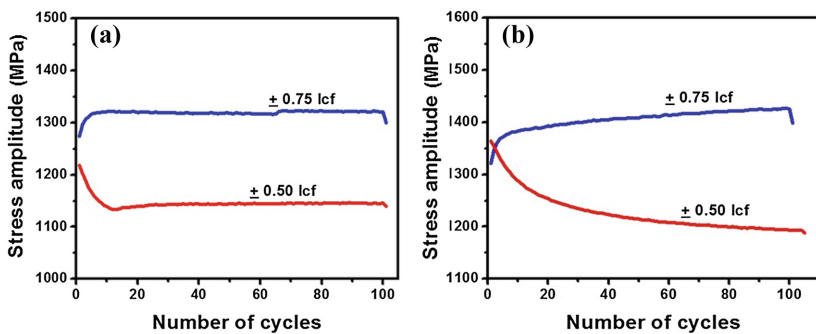

Fig. 6. Obtained stress amplitude values for (a) only low cycle fatigue and (b) after ratcheting low cycle fatigue.

4 Conclusions

In this investigation, the ratcheting behaviour of AISI 4340 steel was investigated under the influence of different stress ratios at room temperature. Post-ratcheting low cycle fatigue tests were also carried out to understand the effect of ratcheting deformation on fatigue behaviour of the steel. The obtained results and their pertinent analyses assist to infer the following major conclusions:

1. Accumulation of ratcheting strain increased with increasing stress ratio in both annealed and normalised specimens of AISI 4340 steel. Maximum accumulation of ratcheting strain (1.16% for annealed and 1.02% for normalised) was observed at $R = -0.4$. Rate of strain accumulation however, decreased from first cycle to last cycle. The reduction in hysteresis loop area was also noticed. This indicated that the selected material is cyclically hardenable in nature.
2. The increase in strain accumulation might be the consequence of variation in remnant dislocation density in the deformed specimens. The dislocation density supposed to be maximum when $R = -0.4$ due to lowest extent of dislocation annihilation.
3. Post ratcheting low cycle fatigue tests showed that the stress amplitude increased for these specimens compared to the only LCF specimens. The fact could be attributed to the previous cyclic hardening during ratcheting tests.

References

1. Farahani, A.V.: Fatigue–ratcheting damage assessment of steel samples under asymmetric multiaxial stress cycles. Theoret. Appl. Fract. Mech. **73**, 152–160 (2014)
2. Xia, Z., Kujawski, D., Ellyin, F.: Effect of mean stress and ratcheting strain on fatigue life of steel. Int. J. Fatigue **18**(5), 335–341 (1996)
3. Steiner, R.: ASM Handbook, Volume 1: Properties and Selection: Irons, Steels and High-Performance Alloys, pp. 1124–1131 (1990)
4. Dutta, K., Ray, K.K.: Ratcheting strain in interstitial free steel. Mater. Sci. Eng. A **575**, 127–135 (2013)
5. Dutta, K., Ray, K.K.: Ratcheting phenomenon and post-ratcheting tensile behaviour of an aluminum alloy. Mater. Sci. Eng. A **540**, 30–37 (2012)
6. Kreethi, R., Mondal, A.K., Dutta, K.: Ratcheting fatigue behaviour of 42CrMo4 steel under different heat treatment conditions. Mater. Sci. Eng. A **679**, 66–74 (2017)
7. Mahato, J.K., De, P.S., Sarkar, A., Kundu, A., Chakraborthi, P.C.: Effect of testing mode on ratcheting and post-ratcheting tensile properties of annealed OFHC copper. Procedia Mater. Sci. **5**, 1358–1367 (2014)
8. Divya Bharathi, K., Dutta, K.: Stress ratio effect on ratcheting behavior of AISI 4340 steel. In: IOP Conference Series: Materials Science and Engineering, vol. 115 (2016). https://doi.org/10.1088/1757-899x/115/1/012016
9. E8M-12: Annual Book of ASTM Standards, Standard Test Method for Tension Testing of Metallic Materials (Metric). ASTM International, West Conshohocken (2012)
10. E606M-12: Standard Test Method for Strain-Controlled Fatigue Testing. ASTM International, West Conshohocken (2012)

11. E112: Standard Test Methods for Determining Grain Size, ASTM International, West Conshohocken (2012)
12. Kang, G., Gao, Q., Yang, X.: A visco–plastic constitutive model incorporated with cyclic hardening for uniaxial/multiaxial ratcheting of SS304 stainless steel at room temperature. Mech. Mater. **34**, 521–531 (2002)
13. Zhang, Y., Hu, C.L., Zhao, Z., Li, A.P., Xu, X.L., Shi, W.B.: Low cycle fatigue behaviour of a Cr–Mo–V matrix-type high-speed steel used for cold forging. Mater. Des. **44**, 612–621 (2013)
14. Yoshida, F.: Uniaxial and biaxial creep-ratcheting behavior of SUS304 stainless steel at room temperature. Int. J. Press. Vessels Pip. **44**, 207–223 (1990)
15. Paul, S.K., Sivaprasad, S., Dhar, S., Tarafder, S.: Ratcheting and low cycle fatigue behavior of SA333 steel and their life prediction. J. Nucl. Mater. **401**, 17–24 (2010)
16. Branco, R., Costa, J.D., Antunes, F.V.: Low-cycle fatigue behaviour of 34CrNiMo6 high strength steel. Theoret. Appl. Fract. Mech. **58**, 28–34 (2012)
17. Zhu, R., Cai, X., Wu, Y., Liu, L., Ji, W., Hua, B.: Low-cycle fatigue behavior of extruded Mg–10Gd–2Y–0.5Zr alloys. Mater. Des. **53**, 992–997 (2014)